



## **Evaluation of Half-Bridge Resonant Inverter Topologies** **Yarım Köprü Rezonans Tipi Evirgeç Topolojilerinin** **Değerlendirilmesi**

**Yıldırım Başkurt** <sup>1\*</sup>, **Haldun Karaca** <sup>2</sup>

<sup>1</sup> Department of Electrical & Electronics Engineering, Dokuz Eylül University, Tınaztepe Campus, 35370, Buca, İzmir, TURKEY

<sup>2</sup> Department of Electrical & Electronics Engineering, Dokuz Eylül University, Tınaztepe Campus, 35370, Buca, İzmir, TURKEY

Sorumlu Yazar / Corresponding Author \*: [yildirimbasakurt@hotmail.com](mailto:yildirimbasakurt@hotmail.com)

Geliş Tarihi / Received: 20.09.2019

Kabul Tarihi / Accepted: 14.01.2020

*Atıf şekli/How to cite: BASKURT, Y., KARACA, H.(2020). Evaluation of Half-Bridge Resonant Inverter Topologies. DEÜFMD 22(65) 505-515.*

Araştırma Makalesi/Research Article

DOI: 10.21205/deufmd.2020226518

### **Abstract**

Resonant power inverters are widely used in today's power electronic industry due to their high efficiencies. These high efficiencies are the result of operating the inverters in either zero current switching (ZCS) or zero voltage switching (ZVS) modes. Although there are many topologies available, the majority of them are mainly derived from two basic structures called "the voltage source series resonant" and "the current source parallel resonant" type inverters. Both inverter topologies incorporate full bridge and half-bridge circuit variations. In this paper, the half-bridge type of series and parallel resonant inverters are investigated. A comparison between the two types - with respect to practical applications - is also presented. Analytically derived results are compared against experimental measurements for two prototypes. Specifically, an 80 kVA half-bridge series resonant and a 3kVA half-bridge parallel resonant type induction heating supplies are being compared. At the end of the study, a detailed comparison table was introduced to the literature.

**Keywords:** : Half-Bridge Inverter, Resonant Inverters, Snubber Circuits, Induction Heating.

### **Öz**

Rezonans güç evirgeçleri, günümüz güç elektroniği endüstrisinde, yüksek verimleri nedeniyle yaygın olarak kullanılmaktadır. Bu yüksek verim evirgeçlerin sıfır akım anahtarlama (ZCS) veya sıfır gerilim anahtarlama (ZVS) modlarında çalıştırılmasının sonucudur. Her ne kadar birçok topoloji mevcut olsa da, bunların çoğu temel olarak "gerilim kaynaklı seri rezonans" ve "akım kaynaklı paralel rezonans" tipi evirgeçler olarak adlandırılan iki temel yapıdan türetilmiştir. Her iki evirgeç topolojisi, tam köprü ve yarım köprü devre varyasyonlarını içerir. Bu çalışmada, seri köprü tipi ve paralel rezonans evirgeçler incelenmiştir. İki tip arasında - pratik uygulamalara göre - bir karşılaştırma da sunulmuştur. Analitik olarak elde edilen sonuçlar, iki prototip üzerinde deneysel ölçümlerle karşılaştırılmıştır. Özel olarak, 80 kVA'lık bir yarım köprü serisi rezonansı ve 3 kVA'lık bir yarım köprü paralel rezonans tipi indüksiyon ısıtma kaynakları incelenmiş ve detaylı bir karşılaştırma tablosu literatüre kazandırılmıştır.

**Anahtar Kelimeler:** Yarım Köprü Evirgeç, Rezonans Evirgeç, Bastırma Devresi, İndüksiyon ile Isıtma.

**1. Introduction**

In order to achieve a size reduction of the power supplies intended for use in modern power electronic systems, it is desirable to increase the operating frequency. This may be achieved by reducing the size of the reactive components. More importantly a specific application may require the need to operate at higher frequencies; for example, the induction heating process. To reduce the higher switching losses resulting from the higher operating frequency, zero current (ZCS) or zero voltage (ZVS) switching inverter topologies have been developed [1]. Although both inverter types generally satisfy basic operating requirements, they have advantages and disadvantages with respect to the application each one is used for. Therefore, depending on the desired application, the selection of the proper type of inverter is of particular importance.

**2. Material and Method**

**2.1. Half-bridge voltage source series resonant inverter**

A schematic diagram for the well-known half-bridge series resonant inverter topology is illustrated in Figure 1. A 80 kVA load power prototype with an operating frequency of around 8.5 kHz was realized. This topology was used in practice for induction surface hardening purposes.

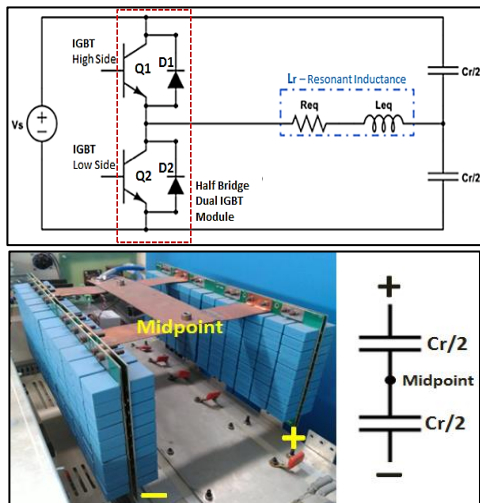


**Figure 1.** TOP: Simplified circuit diagram of the Half-Bridge Series Resonant Inverter realised using IGBT Transistors. BOTTOM: Wiring of the resonant capacitors ( $C_r/2$ ).

Here, the series  $L_r$  (Resonant Inductance) is the equivalent inductance seen from the primary winding of the matching transformer, while the working coil was connected to the secondary winding of the transformer. The resonant capacitors ( $C_r/2$ ) were implemented by connecting small size MKT type capacitors. The practical limitations of the designed capacitor blocks restrict the maximum operating voltage to a value of 3kV. In addition, the maximum current value per capacitor should not exceed 2.5Arms. Therefore, in order to satisfy the 80kVA power requirement of the inverter, 480 pieces of small type MKT capacitors (0.1uF/1600VDC) were used to form the resonant tank capacitor.

The power control was provided by a six-pulse thyristor rectifier. The output voltage of the rectifier is fed to a bulk DC capacitor bank through a serial DC choke, required for this operation. The serial DC choke ensures that during each thyristor firing instant, a huge inrush current is not drawn by the capacitor block. Previous experience showed that the design of the DC capacitor bank generally requires significant attention.

In the voltage source serial resonant inverter topologies, the leakage path inductance from the DC source to the inverter switching components must be as low as possible. This is necessary to eliminate high voltage peaks that may occur during the switching instants as a result of the high current values drawn by the DC supply. If any leakage inductance on this path occurs, a high level of voltage peak will be created. This will result in a failure of the switching components. To avoid this, two major implementations were used in the design [2, 3]:

- i-* The DC current paths and the DC capacitor bank were designed in a layer type structure as shown in Figure 2.
- ii-* A de-coupling capacitor was added as a snubber circuit onto the power supply terminals (C1 and E2) of the half-bridge IGBT module.

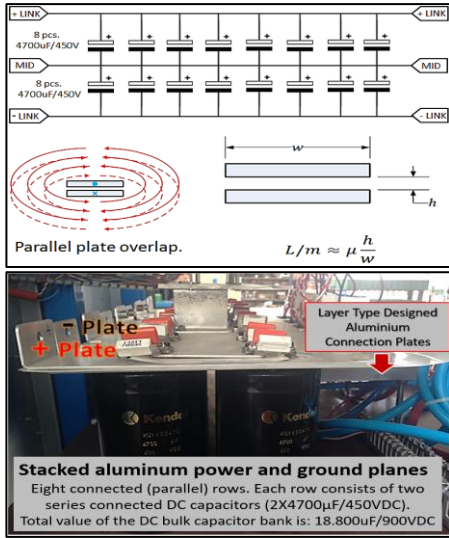
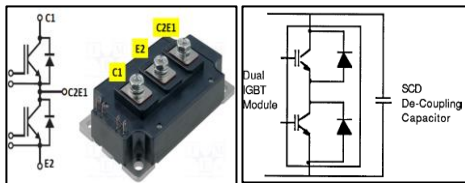
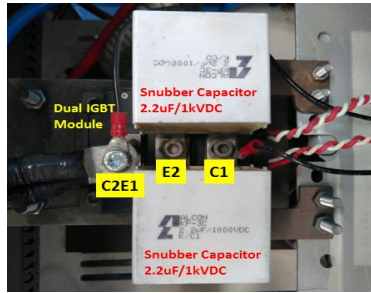


**Figure 2.** TOP: Illustration of the DC capacitor bank. The parallelization was achieved by stacking the power and ground planes, in order to minimize the stray inductance, BOTTOM: Photo of the DC capacitor bank.



(a)



(b)

**Figure 3.** (a) IGBT module terminal illustration, (b) Placement of the de-coupling snubber capacitors.

In the realized 80kVA induction heating system, a 600A/1200V IGBT module (CMY600N1200) from Mitsubishi (Figure 3a) and two 2.2 uF/1kVdc snubber capacitors from Alkon were used (Figure 3b).

Using the internal anti-parallel diodes in each IGBT, the excess voltage that might go over the DC supply is clamped to the maximum rail voltage. This excess voltage may appear due to reverse current passing through the wiring inductances. Therefore, a snubber capacitor with a high  $dv/dt$  rating was placed as close as possible on the IGBT terminals as shown in Figure 3b.

**2.1.1 Operating below resonance**

When the operating frequency is below the load resonant frequency,  $f < f_0$ , the series resonant load behaves as a capacitive load. Three detrimental effects occur during the turn-on phase of an IGBT switch in this case [4]:

- i-Reverse recovery of the anti-parallel diode of the opposite switch.
- ii-Discharging of the transistor output capacitance.
- iii- Miller’s effect caused by Drain to Source capacitance of the IGBT during its turned-on phase.

The most severe drawback during the operation below resonance (for all series resonant inverter variant topologies) is the diode reverse recovery stress. Reverse recovery current spikes are seen in Figure 4 (twice every period).

If the operation of the resonant inverter (voltage source or current-fed type) includes reverse recovery phases for the power diodes, the inverter becomes less reliable and its efficiency also decreases. In almost all cases, reverse recovery phenomena reduce the reliability for all power electronic circuits. The reverse recovery current peaks may reach excess values, which in turn (together with wiring inductances) may cause a serious stress to the diodes or other semiconductor switches. (Wiring inductances induce high voltages when they are forced to cease their current by the turning off of a switch).

The reverse recovery charge that flows from the positive DC supply rail to the negative rail (for the series inverter) or simply through the parallel resonant load capacitor (current-fed inverter) could be expressed as [5];

$$Q_{rr} = I_D \cdot \tau \tag{1}$$

Here  $I_D$  is the forward diode current flowing just before recovery and  $\tau$  is the minority-carrier transit time namely a parameter of the diode. From the beginning of the reverse recovery

process up to the end, the energy loss  $W$  can be expressed as;

$$W = Q_{rr} \cdot V_{DC} \quad (2)$$

Here  $V_{DC}$  is the supply voltage of the inverter. A critical situation called *dynamic avalanche breakdown* [6] might occur at this interval.

The operating frequency of the inverter of Figure 1 is intentionally adjusted below the load resonant frequency value. Consequently, the resulted waveforms seen in Figure 4 clearly show reverse recovery current spikes. These spikes may result to extremely high transient power levels, which together with the wiring inductances during commutation, should be dissipated on the switches.

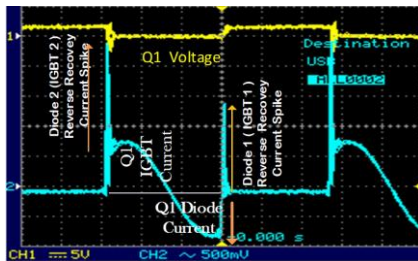


**Figure 4.** Voltage and current waveforms of Switch Q1 of Figure 1. Upper trace (CH1): Q1 Voltage (X50); lower trace (CH2): Q1 current (100mV/A)(during positive IGBT mode current, otherwise the same IGBT’s freewheeling diode’s current).

It is possible to eliminate the reverse recovery problem by operating exactly at the resonant frequency or above the resonance frequency (series resonant inverter), as well as below the resonant frequency (parallel inverter). If these conditions are not met the operation frequency is at the close vicinity of the load resonant frequency. In this condition, the value of  $I_D$  above the resonant frequency is low (the diode current decreases to a low value before driving the gate). Then,  $Q_{rr}$  in equation (2) becomes low and reverse recovery may not pose a serious problem.

On the other hand, IGBTs contain parasitic thyristors inside of their structures. It has been examined that at low current values IGBT failures can occur because for this parasitic component as the inner temperature increases. Any positive feedback effect will lead to the parasitic thyristor being in the on state and causes catastrophic device failures [7]. The new

*Silicon Carbide (SiC) power MOSFET devices* which were very promising devices suffer from the same phenomenon [8].

For  $f < f_0$ , the turn-off switching loss is zero, but the turn-on switching loss is not zero. The transistors are turned on at a high voltage. When the transistor is turned on, its output capacitance is discharged, causing a switching loss. The turn-on switching loss per transistor can be expressed as:

$$P_{ton} = \frac{1}{2} f C_{out} V_i^2 \quad (3)$$

$f$ : Switching frequency

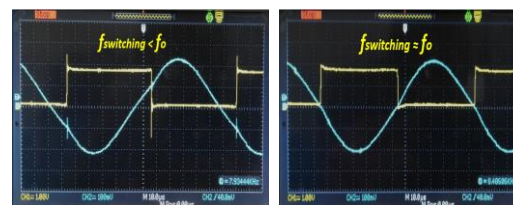
$C_{out}$ : Output capacitance of the transistor

$V_i$ : Transistor C-E voltage at the switching instant.

Another effect that should be considered at the turn-on effect of the transistor is the Miller’s effect. Since the gate-source voltage increases and the collector-emitter voltage decreases during the turn-on transition, Miller’s effect is significant. As a result, the transistor input capacitance increases and the gate drive charge and power requirements also increase, thus reducing the turn-on switching speed.

### 2.1.2 Operating above resonance

Under this operating condition presented in Figure 5, the conduction sequence of the semiconductor devices is D1-Q1-D2-Q2. The transistors (Q1 and Q2) are turned on at zero voltage each time. In fact, there is a small negative voltage across the anti-parallel diode, but this is negligible in comparison to the input voltage  $V_i$ . Therefore, the turn-on switching loss is eliminated and thus Miller’s effect is absent. The diodes turn on at very low  $di/dt$ . For this operation, anti-parallel diodes may react slowly for  $f > f_0$ , the turn-on switching loss becomes zero, but there is a turn-off loss in the transistor due to the wiring inductances.



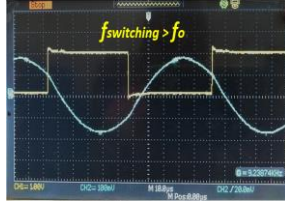


**Figure 5.** Output voltage of Q1 and resonant current waveforms corresponding to the three operational modes: TOP LEFT: for  $f < f_0$ ; TOP RIGHT: for  $f \approx f_0$  and BOTTOM: for  $f > f_0$  (CH1: X200, CH2: 10mV/A)

Considering the above discussion, the operating frequency ( $f$ ) of the realized inverter was tuned at a slightly higher value than the resonant load frequency ( $f_0$ ), to ensure it never drops below the load resonance frequency during the transients.

### 2.1.3 Setting the “dead” time

Since totem-pole connected IGBT pairs in a series inverter are being energized by a voltage source of a power supply, a sufficient enough “dead” time is required during the switching intervals to ensure that the IGBTs are never both in conduction at any one instant. If, however, the “dead” time is set too long, the commutated current level somehow acquires higher values. This may result in increasing losses. In the specific application realized, the “dead” time was set to  $3\mu\text{s}$  when the operating frequency was about 10 kHz. This value was checked in practice.

### 2.1.4 Operating parameters of series resonant load

- Loaded quality factor:

$$Q_L = \frac{L\omega_0}{R} = \frac{1}{\omega_0 CR} = \frac{Z_0}{R} \quad (4)$$

- Input impedance:

$$Z = Z_0 \sqrt{\left(\frac{1}{Q_L^2} + \left(\frac{\omega}{\omega_0} - \frac{\omega_0}{\omega}\right)^2\right)} \quad (5)$$

$$\Psi = \arctan\left[Q_L \left(\frac{\omega}{\omega_0} - \frac{\omega_0}{\omega}\right)\right] \quad (6)$$

It should be noted that while operating exactly at the resonant frequency ( $\omega = \omega_0$ ), the load impedance will become;

$$Z = \frac{Z_0}{Q_L} \quad (7)$$

Therefore, when working with a series resonant type induction heating system, the work coil should not be left unloaded, as this will increase

the quality factor of the system, causing excessive power drawing from the source. The experimental work confirmed these phenomena indicating that a fast overcurrent control scheme may be a good solution. The operating voltage and current waveforms of the work coil ( $L_r$ ) are given in Figure 6.

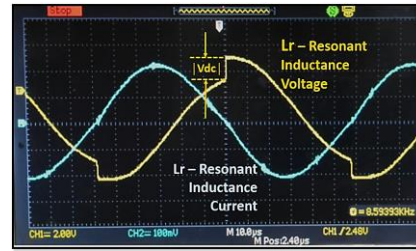


**Figure 6.** Current and voltage waveforms of the resonant inductor of Figure 1. Here,  $L_r$  represents the inductance seen from the primary of the matching transformer. Note that the voltage burst seen at the top of the inductor voltage waveform is the result of the switching occurring just at that time (CH1: X200, CH2: 10mV/A).

## 2.2 Half-bridge current source resonant inverter

All the measurements were taken in a 3kVA-12 kHz current source half-bridge type parallel resonant inverter for the induction heating system prototype as shown in Figure 7. The  $L_{dc\text{-choke1}}$  and  $L_{dc\text{-choke2}}$  coils form a constant current source in combination with the DC power supply. The resonant load is represented by the parallel connection of the work coil  $L$ , the resonant capacitor  $C$  and the work-piece reflected internal resistance  $R$ . Two separate insulated gate drivers (VLA502 from FUJI) were used to separate the power and the control stages, in order to drive the single IGBTs (GD200SGL120C2S from Starpower). The advantages of the half bridge inverter are its simple trigger circuits and the reduction in the number of switches for low and medium power applications in comparison with the full bridge topology. The inductances of  $L_{dc\text{-choke1}}$  and  $L_{dc\text{-choke2}}$  are much larger than the resonant inductor  $L$ , so under normal steady-state operation the dc-link current is approximately constant, and the switching network injects an alternating square-wave current into the resonant tank [9]. In the Literature an interesting application (Power Supply for an induction fluorescent lamp) of the topology depicted in Figure 7. is proposed [10]. The proposed circuit given in the Literature

above uses no resonant frequency tracking scheme. However our experimental set-up uses a control circuitry which accommodates a PLL type resonant tracking scheme in order to tune the inverter to the right operating frequency. The control circuitry design was based on a PLL type resonant tracking system, in order to tune the right operating frequency. This frequency varies with the change of the magnetic properties of the load. On the other hand, the control circuitry ensures the proper setting of the operating frequency with the no-load condition of the inverter. The nature of the topology allows the current source resonant type inverters to operate without load, thus consuming much less power than their nominal ratings. This property provides a significant advantage against other topologies (see Table 1).

In high voltage IGBTs the overcurrent turn-off capability is an important design feature which characterizes the ability of a device to switch-off from an overload condition safely. In general such an event moves the device to the edge of its safe operating area (SOA), connected with the appearance of large avalanche generated currents [11].

During the design stage this issue has to be taken into consideration carefully since the switching always occurs at high current levels in current source parallel resonant inverters.

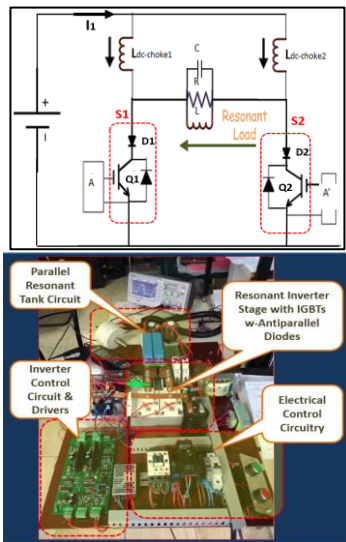
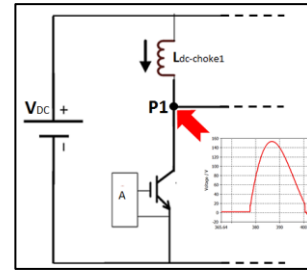
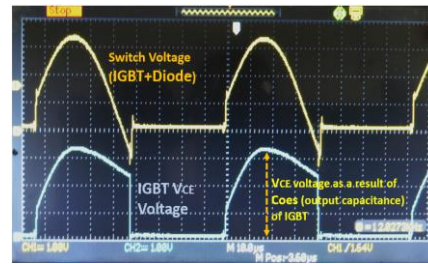


**Figure 7.** Circuit diagram of the 3kVA/12kHz Half-Bridge Parallel Resonant Inverter and its corresponding prototype.



(a)



(b)

**Figure 8.** (a) Schematic illustration of the measurement node P1 (voltage across the collector (C) and the emitter (E) terminals of the single IGBT), (b) Measured switch voltage waveforms (Upper Trace: IGBT+Diode Voltage waveform, Lower Trace: IGBT Voltage waveform (CH1:X200, CH2: X200)).

It has been simulated and measured that the peak collector voltage can go up to “ $\pi$ ” times the value of the applied DC supply voltage (Figure 8, (a) and (b) respectively). This is because the average voltage values between the terminals of the  $L_{dc}$ -choke coil must be equal in the steady-state case. Therefore;

$$V_{dc} = V_{Ldc} \frac{1}{2\pi} \left[ \int_0^{\pi} \sin \omega t \cdot dt + \int_{\pi}^{2\pi} 0 \cdot dt \right] \quad (8)$$

$$V_{dc} = \pi \cdot V_{dc} \dots (\text{max. value}) \quad (9)$$

In practice, this may lead to a serious problem. If the DC supply voltage is obtained by rectifying the mains voltage (which is about 230Vrms), then the DC voltage is about 320V. Consequently, the collector voltage of the IGBT’s can go up to  $\pi \times 320 = 1.020 V_{peak}$ . Therefore, can be concluded that this scheme requires switches able to withstand higher voltage levels when compared with its series inverter counterpart.

### 2.2.1. Operation below resonance

For  $f < f_0$ , the parallel resonant circuit behaves as an inductive load. Under this operating condition at the end of the switching sequences, the capacitor  $C_{out}$  is discharged through the

transistor, resulting in turn-on switching loss in the IGBT. This can be expressed as:

$$P_D \approx f C_{out} V^2_{SM} / 2 \tag{10}$$

This energy is fixed and independent of the load current. For high frequency or high voltage operation, this loss may prove to be a limit with respect to the size of the snubber capacitor employed [12].

**2.2.2. Operation above resonance**

For  $f > f_0$ , the parallel resonant circuit represents a capacitive load. Hence, the voltage across the resonant circuit lags behind the fundamental component of the tank circuit feed current by the phase angle  $\psi$ . The switch begins the off-state with a negative voltage and ends with a positive voltage. The IGBTs experience “soft” switching and zero turn-off switching loss, while the series diodes experience zero turn-on switching loss. However, there is a turn-on switching loss in each IGBT and reverse recovery turn-off loss in each series diode. For these two reasons, the efficiency above resonance is less than that below resonance.

MIDDLE: for  $f \approx f_0$  and BOTTOM: for  $f > f_0$  (CH1:X200, CH2: 100mV/A).

As discussed before, there a significant effect occurs during the switching-off period of the semiconductor devices due to the “reverse recovery” behaviour of the diodes. In a current source parallel resonant inverter, the reverse recovery causes the output resonant tank circuit to be short-cut during the reverse recovery interval as illustrated in Figure 10. This type of operation occurs when the inverter is operated above the load resonant switch. It should be noted that reverse recovery currents are enormously high and can only be limited by the short-circuit path impedance, which is very low especially in high power inverter structures. This current path has to be also as low inductive as possible in order not to cause any over voltage shoots during the switching instants.

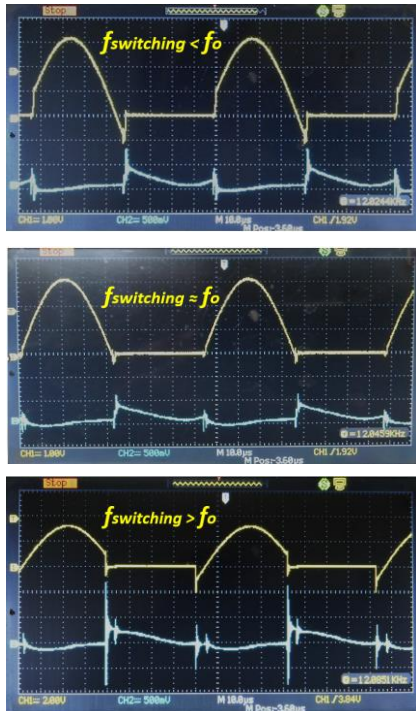


**Figure 9.** Output voltage of Switch-1 (Q1+D1) and resonant current waveforms, corresponding to three operational modes: TOP: for  $f < f_0$ ;

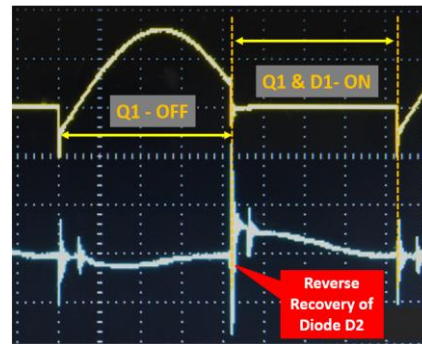
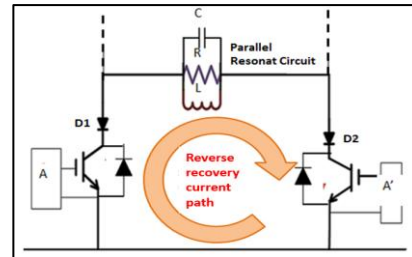


**Figure 10.** Reverse recovery current path in the current source resonant inverter. (The voltage across the terminals of the resonant capacitor works as a source for the reverse recovery current). Reverse recovery current peaks occurring on the switch current waveform at the switching instant, while being operated above the resonant frequency of the load (Upper trace: Voltage between the terminals of S1 in Figure 7; Lower trace: Current passing through S1 in Figure 7).

### 2.2.3. Setting the overlap-time

In order for the DC choke coils not to be left open-circuited at the switching instants, there must be an overlapping time period at the drive signals. This overlap time should not be too long, as it directly reduces the efficiency of the inverter. In the application set-up, an overlap time of around 1µs was set at a 12 kHz operating frequency at the IGBT driver side.

### 2.3. Operating parameters of a parallel resonant load

- Resonant frequency:

$$\omega_0 = \frac{1}{\sqrt{LC}} \quad (11)$$

- Characteristic impedance:

$$Z_0 = \sqrt{\frac{L}{C}} = \omega_0 L = \frac{1}{C\omega_0} \quad (12)$$

- Loaded quality factor:

$$Q_L = \omega_0 CR = \frac{R}{\omega_0 L} = \frac{R}{Z_0} = \frac{1}{GZ_0} \quad (13)$$

- Input admittance:

$$Y = \frac{I_{rms}}{V_{rms}} = \frac{1}{Z_0} \sqrt{\left(\frac{1}{Q_L^2} + \left(\frac{\omega}{\omega_0} - \frac{\omega_0}{\omega}\right)^2\right)} \quad (14)$$

$$\Psi = \arctan\left[Q_L \left(\frac{\omega}{\omega_0} - \frac{\omega_0}{\omega}\right)\right] \quad (15)$$

$V_{rms}$ : rms value of the ac output voltage of the inverter.

$I_{rms}$ : rms value of the fundamental component of the resonant circuit input current.

It should be noted that while the parallel inverter operates at the resonant frequency of the load, the load admittance may be expressed as;

$$Y = \frac{1}{Q_L Z_0} \quad (16)$$

This expression dictates that at higher  $Q_L$  values, the load admittance value of the parallel resonant inverter will be smaller in magnitude, or in other words the load impedance will be higher. Therefore, in a parallel resonant type induction heating system, the work coil can safely be left unloaded, as this will increase the quality factor of the system, causing minimum current demand from the power source.

### 3. Results

So far, the operation and the related parameters of the series and parallel half-bridge resonant inverters have been discussed and examined. Comparing the nature of both topologies, some

important differences between them may be noticed. These differences must be taken into account when choosing the proper inverter type, depending on the particular application. The change of load parameters is an inevitable effect in an induction heating system.

The load parameters relative magnetic permeability ( $\mu_r$ ) and electrical resistivity ( $\rho$ ) change rapidly depending on the temperature of the load. Thus, the change of these properties affects two fundamental design parameters of the inverter: the operating frequency and the load matching circuitry.

Great care should be taken while setting the right operating frequency, depending on the inverter type and also on the change of the load parameter,  $\mu_r$ . This parameter decreases (if the load is made of ferromagnetic material) with the increase in temperature of the heated work-piece, and becomes equal to "1" after the Curie temperature. The second issue concerns the design of the output matching circuitry. In practical applications, this is generally done using a matching transformer. In an induction heating system,  $\rho$  increases as the work-piece becomes hotter causing the load resistance to increase. This means the inverter sees a "light" load at higher temperatures. Therefore, this effect causes a series resonant type inverter to demand extremely high current values. A fast power control circuit is designed as a solution to this problem. Apart from these two basic concerns, there are several parameters that need to be taken into account while choosing the appropriate inverter topology, depending on the specific application. In the Table 1, a summary including theoretical and experimental research results is presented. The abbreviation VSHBSRI refers to "voltage source half-bridge series resonant inverter", while CSHBPRI refers to "current source half-bridge parallel resonant inverter".

In addition to the above points of concern, high frequency operation of the inverters makes circuit systems compact with smaller passive components. However, ringing occurs at high-speed switching because voltage and current steeply fluctuate during switching. Ringing induces electromagnetic interference (EMI) noise and malfunction, which threatens reliability. Thus, it is necessary to address ringing especially at higher operating frequencies. The discharge-suppressing resistor-capacitor-diode (RCD) is commonly used for this purpose [13].

**Table 1.** Comparison of the studied inverter structures

Comparison Parameters	VSHBSRI		CSHBPRI	
Soft Switching Behavior	Zero-current switching at resonance	↔	Zero-voltage switching at resonance	↔
Switch Voltage - $V_{peak}$	$V_{dc}$	↑	$\pi V_{dc}$	↓
Switch Current – $I_{peak}$ (Note 1)	$2I_{dc}$	↓	$I_{dc}$	↑
Switch Voltage Waveform	Square Wave	↔	Sinus wave	↔
Switch Current Waveform	Sinus wave	↑	Square wave	↓
Proper Operating Frequency Setting (Note 2)	$f_{switching} \geq f_{resonant}$	↔	$f_{switching} \leq f_{resonant}$	↔
No Load Operation	Max. Switch Current	↓	Min. Switch Current	↑
Switch Construction	only IGBT			↑
Critical Current Path (Note 3)	Between DC supply and the Switch	↔	Diode + IGBT combination	↓
Recommended Snubber Type	A simple snubber capacitor between DC rails on the switches gives sufficient result.	↑	Between Switch and the Resonant Tank	↔
Gate Drive Requirement	Dead Time is required	↔	More complicated RCD type snubbers are recommended across the switches.	↓
Power Line Interruption Sensitivity	No additional precaution is required.	↑	Overlap is required	↔
Driver Selection	Proper gate drivers including fast overcurrent/short circuit detection circuits have to be chosen.	↔	Gate drives must continue to operate; in case of failure a special crowbar circuitry has to be placed.	↓

↑: Advantage, ↓: Disadvantage, ↔: Not a superior item.

(Note 1):  $I_{dc}$  refers to the current drawn from the DC power source. Assuming  $I_{dc} = V_{dc}/R$  note that;

In mono-phase power network:  $V_{dc} = (2\sqrt{2}/\pi) \cdot V_{i_{rms}}$ , ( $V_{i_{rms}}$  is the line to neutral voltage).

In three-phase power network:  $V_{dc} = (3\sqrt{2}/\pi) \cdot V_{phase_{rms}}$ , ( $V_{phase_{rms}}$  is the rms value of the line-to-line voltage).

(Note 2): Have to be set just "slightly" over or lower of the natural resonant frequency depending on the inverter type.

(Note 3): The leakage inductance of these paths have to be designed as low as possible.

#### 4. Discussion and Conclusion

An experimental study was carried out on two well-known resonant inverter topologies. Half-bridge series and parallel resonant structures were analyzed and key real time measurements were performed on the implemented systems. Their operation was studied while operating lower, over and at the natural resonant frequency of the load. Practical limitation concerns were pointed out and dealt with.

The work carried out during prototyping and the results of the tests for the current-fed inverter showed the importance of properly wiring power stage switches to each other and to DC supply rails. It is theoretically known that parasitic wiring inductances are unavoidable. However, minimizing these stray inductances is more crucial for current-fed inverters than for series-type inverters. This is because switching occurs at small current levels in series inverters. However, in parallel-type inverters, current levels are large at the instance of switching, which induces larger energy levels in wiring inductances. This energy must then be dissipated in the switch during its turning off.

During the study involving the parallel resonant inverter, we faced several device failures even when working at load resonant frequency. We concluded that the above mentioned wiring inductances carry high currents that are forced to drop to zero by the wired IGBT's. Then, unclamped inductive switching occurs, which leads the semiconductor switches to failures. It can be claimed that an elaborately designed turn-off snubber does not simply increase the reliability of the parallel resonant inverter, but is nearly a necessity for proper operation. The power modules available today are almost suitable for series-type inverters. For example, the module given in Figure 3 cannot be used in the parallel inverter topology studied in this work. On the other hand, when discrete power switches are wired in parallel type inverter topologies, extra wiring elements (bus-bars, cables or plates) are necessary. These elements in turn substantially increase the wiring inductances.

A detailed comparison table was presented, in order to point out the advantages and disadvantages of both inverter types against each other. The study showed that the choice of the inverter topology is mainly related to the application requirements; however, the series

resonant type structures are somehow more reliable. The reason for this is, the switching occurs at small current levels in series inverters. But in parallel type inverters the current levels are large at the switching instants causing larger energy levels to appear in wiring inductances.

#### ACKNOWLEDGMENT

Foremost, I would like to express my sincere gratitude to my advisor Prof. Dr. Haldun Karaca for the continuous support of my research, for his patience, motivation, enthusiasm, and immense knowledge. His guidance helped me in all the time of research and writing of this paper. Besides this, I would also like to express my special thanks to the employees of Guclu Induction Co. for their effective and sincere support during my research.

#### REFERENCES

- [1] Dieckerhoff, S., Ryan, M.J., Doncker, R.W. 1999. Design of an IGBT-based LCL-Resonant Inverter for High Frequency induction Heating. IEEE 34th Industry Applications Conference, 3-7 October, Phoenix, AZ, USA, 2039-2045.
- [2] CREE Inc. 2013. Design Considerations for Designing with Cree SiC Modules Part 1. Understanding the effects of parasitic inductance CPWR-AN12. Durham, NC, USA: Cree.
- [3] CREE Inc. 2013. Design Considerations for Designing with Cree SiC Modules Part 2. Techniques for minimizing parasitic inductance CPWR-AN13. Durham, NC, USA: Cree.
- [4] Kazimierczuk, M.K., Czarkowski, D. 2011. Resonant Power Converters. 2nd ed. New Jersey, USA: John Wiley & Sons Inc., p. 149-157, p.309-315.
- [5] Dimitrijević, S. 2011. Principles of Semiconductor Devices. 2nd ed. Oxford, United Kingdom: Oxford University Press, p. 239-241.
- [6] Linder, S. 2006. Power Semiconductors. 1st ed. Lausanne, Switzerland: EPFL Press, p 83-85.
- [7] Lu, J., Tian, X., Lu, S., Zhou, H., Zhu, Y., Han, Z. 2013. Dynamic Avalanche Behavior of power MOSFETs and IGBTs under Unclamped Inductive Switching Conditions, Journal of Semiconductors, Volume 34, No 3, 5. doi:10.1088/1674-4926/34/3/034002.
- [8] Na Ren, Kang L. Wang Jiupeng Wu, Hongyi Xu, Kuang Sheng. 2019. Failure Mechanism Analysis of SiC MOSFETs in Unclamped Inductive Switching Conditions, Proceedings of the 31st International Symposium on Power Semiconductor Devices & ICs, 19-23 May, Shanghai, China, 183-186.
- [9] Namadmalan, A., Moghani, J.S., Milimonfared, J.A. 2011. A Current-Fed Parallel Resonant Push-Pull Inverter with a New Cascaded Coil Flux Control for Induction Heating Applications, Journal of Power Electronics, Volume 11, No. 5, p.632-638.
- [10] Oscar M. Rodríguez-Benítez ; Mario Ponce-Silva ; Juan Antonio Aquí-Tapia ; Claudia Cortés-García. 2018. Resonant Half-Bridge Current-Inverter (RHBCI) used as Power Supply for Induction Lamps with High-Power-Factor and without Electrolytic Capacitors. IEEE 14th International Conference on Power Electronics (CIEP) Conference, 24-26 October, Puebla, Mexico, 56-61.
- [11] Phillipou, A., Jaeger, C., Laven, J.G., Baburske, L., Shultz, H. J., Pfirsch, F., Niedernosthede F. J., Vellei, A., Itani, H. Critical Over Current Turn-off Close to IGBT Current Saturation: Proceedings of 27th International Symposium

of Power Semiconductor Devices & ICs, May 10-14, 2015, Kowloon, Hong Kong, 113-116.

[12] Stephen, J.F., Barry, W., Green, T.C. 1996. RCD Snubber Revised, IEEE Transactions on Industry Applications, Volume 32, p.155-160.

[13] Yamashita, Y., Furuta, J., Inamori, S., Kobayashi, K. 2017. Design of RCD Snubber Considering Wiring Inductance for MHz-switching of SiC-MOSFET. IEEE 18th Workshop on Control and Modeling for Power Electronics (COMPEL), 9-12 July, Stanford, CA, USA